UC Berkeley
SEMM Reports Series

Title
Thick Shell and Solid Finite Elements With Independent Rotation Fields

Permalink
https://escholarship.org/uc/item/0002x3n1

Authors
Ibrahimbegovic, Adnan
Wilson, Edward

Publication Date
1989-12-01

eScholarship.org Powered by the California Digital Library
University of California

LOAN COPY

PLEASE RETURN TO
NISEE/Computer Applications
404A Davis Hall
(415) 642 - 5113

REPORT NO.
UCB/SEMM 89/25

STRUCTURAL ENGINEERING,
MECHANICS AND MATERIALS

THICK SHELL AND SOLID FINITE ELEMENTS WITH INDEPENDENT ROTATION FIELDS

By:

ADNAN IBRAHIMBEGOVIC

and

EDWARD.L. WILSON

DECEMBER 1989

DEPARTMENT OF CIVIL ENGINEERING
UNIVERSITY OF CALIFORNIA
BERKELEY, CALIFORNIA

THICK SHELL AND SOLID FINITE ELEMENTS WITH INDEPENDENT ROTATION FIELDS

Adnan Ibrahimbegovic[†] and Edward L. Wilson[‡]

Department of Civil Engineering, University of California, Berkeley, CA 94720, U.S.A.

ABSTRACT

Thick shell and solid elements presented in this work are derived from variational principles employing independent rotation fields. Both elements are built on a special hierarchical interpolation and both possess six degrees of freedom per node. Performance of the elements is evaluated on a set of problems in elastostatics. However, the formulation presented herein is also suitable for transient and nonlinear problems.

† Assistant Research Engineer

‡ Professor

TABLE OF CONTENTS

THICK SHELL AND SOLID FINITE ELEMENTS WITH INDEPENDENT ROTATION FIELDS

Adnan Ibrahimbegovic† and Edward L. Wilson‡

Department of Civil Engineering, University of California, Berkeley, CA 94720, U.S.A.

1. INTRODUCTION

The early approach to finite element analysis of plates and shells utilized Kirchhoff thin plate theory. However, this approach is appropriate only if the transverse shear deformations are disregraded. More important deficiency of the Kirchhoff thin plate theory, in the finite element context, is the need to impose C^1 shape function continuity, i.e. continuity across the element boundaries is required for both the shape functions and their derivatives. More recent works (e.g., see Bathe & Dvorkin [1985], Hughes & Tezduyar [1981], Tessler & Hughes [1983], Zienkiewicz et al. [1989]) have turned to Reissner [1945] - Mindlin [1951] plate theory as a starting point of finite element discretization. In this case only C^0 shape function continuity is required, hence an interpolation field is more easily constructed.

In Reissner-Mindlin plate theory, an independent rotation field is introduced to describe plate flexural motion. Similarly, a three-dimensional continuum mechanics problem can be formulated with the variational principle which employs an independent rotation field. In this formulation, first given by Reissner [1965], the symmetry of the stress tensor is not a priori enforced. The skew-symmetric part of the stress tensor appears as a Lagrange multiplier for enforcing the equality of the independent rotation field to the skew-symmetric part of displacement gradient.

---

† Assistant Research Engineer

‡ Professor

The Reissner's variational principle can be used as a basis for a new formulation for the plane problems with drilling rotation fields, as shown by Hughes & Brezzi [1989] and Hughes et al. [1989]. Hughes & Brezzi [1989] have also shown that Reissner's variational principle needs to be regularized in order to preserve stability of the discrete finite element approximation. These developments are in a sharp contrast with the previous works on membrane elements with drilling degrees of freedom (e.g., see Allman [1984,87,88], Bergan & Fellipa [1985], Carpenter et al. [1985], MacNeal & Harder [1988], Taylor & Simo [1985]).

The quadrilateral membrane finite element based on regularized Reissner's formulation is presented in our recent work (see Ibrahimbegovic, Taylor & Wilson [1989]). The element is built on a special hierarchical displacement field. In this paper we demonstrate that the same interpolation field can be extended to generate solid elements with rotational degrees of freedom. Similar hierarchical interpolation field can also be successfully used for discretization of the Reissner-Mindlin plate, as well as the adequate thick shell obtained after superposing our membrane elements with drilling degrees of freedom. Solid elements with rotational degrees of freedom presented herein represent an alternative approach to solving thick shell problems. However, their primary value is in serving as a transition from classical structural analysis kinds of models to continuum mechanics models.

By degenerating a quadrilateral thick shell element of this kind, the triangular thick shell element is recovered. The degenerating process is analogous to the one we presented previously (see Ibrahimbegovic & Wilson [1989]). Similarly, it is possible to degenerate the brick solid element presented herein to recover the adequate wedge and tetrahedron solid elements.

The outline of the paper is as follows. In Section 2, we discuss the variational formulation for both the solid and the thick shell elements presented herein. The strong form of both boundary value problems are also stated. The finite element interpolation field is discussed in Section 3. Numerical evaluation for both elements is presented in Section 4. In Section 5, we give some closing remarks.

2. VARIATIONAL FORMULATION

Variational formulations for both the thick shell and the solid problems are given in this section. For the sake of brevity, the discussion of boundary conditions is omitted, i.e. we consider Dirichlet boundary value problem with the zero field variable values over the boundary. Extension to different boundary conditions presents no difficulties for the considerations to follow, and it can be handled in a standard manner (e.g., see Bathe [1982] or Hughes [1987]). We also limit ourselves to linear elastostatic problems.

2.1. Variational Formulation for Three-Dimensional Solids

In this section we follow closely the work of Reissner [1965] and Hughes & Brezzi [1989]. The standard indicial notation is utilized with indices varying over set {1,2,3}. Summation convention on repeated indices is implied. Let Ω be a region occupied by a body. The boundary value problem under consideration is: For *all* $\mathbf{x} \in \Omega$

$$\sigma_{ji,j} + f_i = 0 \tag{2.1}$$

$$skew\ \sigma_{ij} = 0 \tag{2.2}$$

$$\psi_{ij} = skew\ u_{i,j} \tag{2.3}$$

$$symm\ \sigma_{ij} = C_{ijkl}\ symm\ u_{k,l} \tag{2.4}$$

where (2.1) to (2.4) are, respectively, the equilibrium equations, the symmetry conditions for stress tensor $\boldsymbol{\sigma} = \{\sigma_{ij}\}$, the definition of the skew-symmetric rotation tensor $\boldsymbol{\psi} = \{\psi_{ij}\}$ in terms of displacement gradient $\nabla\ \mathbf{u} = \{u_{i,j}\}$, and the constitutive equations. In the usual manner, comma denotes the partial differentiation, i.e. $u_{i,j} = \partial u_i / \partial x_j$.

In (2.1) to (2.4) the Euclidian decomposition of second-rank tensors is employed, e.g.

$$\sigma_{ij} = symm\ \sigma_{ij} + skew\ \sigma_{ij} \tag{2.5}$$

where

$$symm\ \sigma_{ij} = \frac{1}{2}\ (\sigma_{ij} + \sigma_{ji}) \tag{2.6}$$

$$skew\ \sigma_{ij} = \frac{1}{2}\ (\sigma_{ij} - \sigma_{ji}) \tag{2.7}$$

For the isotropic elasticity, the constitutive modulus tensor $\mathbf{C} = \{C_{ijkl}\}$ has the form

$$C_{ijkl} = \lambda\ \delta_{ij}\delta_{kl} + \mu\ (\delta_{ik}\delta_{jl} + \delta_{il}\delta_{jk}) \tag{2.8}$$

where λ and μ are Lame's parameters and δ_{ij} is Kronecker delta.

Reissner [1965] presented a variational formulation for the boundary value problem (2.1) to (2.4). This principle leads to a formulation which is inappropriate for numerical applications. Essentially, too many parameters for the skew-symmetric part of $\boldsymbol{\sigma}$ exist and the numerical problem fails the *LBB* conditions as well as the counts for the mixed patch test (e.g., see Zienkiewicz & Taylor [1989]). Hughes & Brezzi modified variational problem of Reissner by adding the term

$$-\tfrac{1}{2}\ \gamma^{-1} \int_{\Omega} skew\ \sigma_{ij}\ skew\ \sigma_{ij}\ d\Omega \tag{2.9}$$

in order to preserve the stability of the discrete problem. In (2.9), γ is a problem dependent regularization parameter (see Hughes & Brezzi [1989]). For isotropic elasticity and Dirichlet boundary value problem Hughes et al. [1989] suggest γ be taken as shear modulus value, i.e. $\gamma = \mu$. The modification of Reissner's variational formulation preserves (2.1), (2.2) and (2.4) as the Euler-Lagrange equations. In addition, we now have

$$\gamma^{-1}\ skew\ \sigma_{ij} = skew\ u_{i,j} - \psi_{ij} \tag{2.10}$$

If the symmetrical components of stress are eliminated using the constitutive equations (2.4), then the modified variational formulation is given as *Problem (M)*

$$\Pi_{\gamma}(\bar{\mathbf{u}},\bar{\boldsymbol{\psi}},skew\ \bar{\boldsymbol{\sigma}}) = \frac{1}{2} \int_{\Omega} symm\ \bar{u}_{i,j}\ C_{ijkl}\ symm\ \bar{u}_{k,l}\ d\Omega + \int_{\Omega} skew\ \bar{\sigma}_{ij}\ (skew\ \bar{u}_{i,j} - \bar{\psi}_{ij})\ d\Omega$$

$$- \frac{1}{2}\gamma^{-1} \int_{\Omega} skew\ \bar{\sigma}_{ij}\ skew\ \bar{\sigma}_{ij}\ d\Omega - \int_{\Omega} \bar{u}_i\ f_i\ d\Omega \tag{2.11}$$

where $\bar{\mathbf{u}} \in \mathbf{V}$, $\bar{\boldsymbol{\psi}} \in \mathbf{W}$, $skew\bar{\boldsymbol{\sigma}} \in \mathbf{T}$ are spaces of trial displacements, rotations and stresses ($\bar{(\ )}$ denotes the trial variables). This variational formulation requires that the rotations $\bar{\boldsymbol{\psi}}$ and stresses $skew\bar{\boldsymbol{\sigma}}$ together with the displacement generalized derivatives $\nabla\ \bar{\mathbf{u}}$, belong to the space of square-integrable functions over the region Ω, i.e. C^0 continuity is imposed only on displacement field $\bar{\mathbf{u}}$.

The variational equation which results from taking the variations on (2.11) is

$$0 = D\Pi_{\gamma}(\mathbf{u},\boldsymbol{\psi},skew\ \boldsymbol{\sigma}) \cdot (\bar{\mathbf{u}},\bar{\boldsymbol{\psi}},skew\ \bar{\boldsymbol{\sigma}}) = \int_{\Omega} symm\ \bar{u}_{i,j}\ C_{ijkl}\ symm\ u_{k,l}\ d\Omega$$

$$+ \int_{\Omega} skew\ \bar{\sigma}_{ij}\ (skew\ u_{i,j} - \psi_{ij})\ d\Omega + \int_{\Omega} (skew\ \bar{u}_{i,j} - \bar{\psi}_{ij})\ skew\ \sigma_{ij}\ d\Omega$$

$$- \gamma^{-1} \int_{\Omega} skew\ \bar{\sigma}_{ij}\ skew\ \sigma_{ij}\ d\Omega - \int_{\Omega} \bar{u}_i\ f_i\ d\Omega \tag{2.12}$$

In the next section, the variational equation (2.12) is used to construct a mixed-type discrete formulation.

It is possible to eliminate the skew-symmetric part of the stress tensor by substituting (2.10) into *Problem (M)* to obtain *Problem (D)*

$$\tilde{\Pi}_{\gamma}(\bar{\mathbf{u}}, \bar{\boldsymbol{\psi}}) = \frac{1}{2} \int_{\Omega} symm\ \bar{u}_{i,j}\ C_{ijkl}\ symm\ \bar{u}_{k,l}\ d\Omega$$

$$+ \frac{1}{2}\ \gamma \int_{\Omega} (skew\ \bar{u}_{i,j} - \bar{\psi}_{ij})\ (skew\ \bar{u}_{i,j} - \bar{\psi}_{ij})\ d\Omega - \int_{\Omega} \bar{u}_i\ f_i\ d\Omega \tag{2.13}$$

The corresponding variational equation now is

$$0 = D\tilde{\Pi}_{\gamma}(\mathbf{u}, \boldsymbol{\psi}) \cdot (\bar{\mathbf{u}}, \bar{\boldsymbol{\psi}}) = \int_{\Omega} symm\ \bar{u}_{i,j}\ C_{ijkl}\ symm\ u_{k,l}\ d\Omega$$

$$+ \gamma \int_{\Omega} (skew\ u_{i,j} - \bar{\psi}_{ij})\ (skew\ u_{i,j} - \psi_{ij})\ d\Omega - \int_{\Omega} \bar{u}_i\ f_i\ d\Omega \tag{2.14}$$

The variational equation (2.14) is taken as the basis for constructing a displacement-type discrete formulation which is presented in the next section.

2.2. Variational Formulation for Thick Shell

The thick shell element presented herein is obtained by superposing the membrane elements with drilling degrees of freedom and thick plate elements based on Reissner-Mindlin plate theory. The element reference configuration is flat, so that the total potential energy can be split into the membrane and the plate part. A simple nodal computations transforms from flat to warped element configuration. The membrane part is essentially just a subset of the considerations for three-dimensional solids given in Section 2.1. It is discussed in our earlier work (see Ibrahimbegovic, Taylor & Wilson [1989]). The Reissner-Mindlin plate theory, the adequate boundary value problem and its variational formulation is discussed further. The formulation is again given in a standard indicial notation, but the indices now vary over set {1,2}. For the region Ω occupied by the thick plate under consideration, it hold: For *all* $\mathbf{x} \in \Omega$

$$\kappa_{ij} = \beta_{i,j} \tag{2.15}$$

$$\gamma_i = \beta_i + w_{,i} \tag{2.16}$$

$$m_{ij} = C^B_{ijkl}\ \kappa_{kl} \tag{2.17}$$

$$q_i = C^S_{ij}\ \gamma_j \tag{2.18}$$

$$m_{ij,j} - q_i = 0 \tag{2.19}$$

$$q_{i,i} + f = 0 \tag{2.20}$$

where (2.15) to (2.20) are, respectively, the strain-displacement relationship, the constitutive equation and the equilibrium equations. In the equations above, w is the transverse displacement, β_i is a rotation vector of the fiber (director) initially normal to the plate midsurface, κ_{ij} is the curvature tensor, γ_i is the shear strain vector, m_{ij} is a moment tensor, q_i is the shear force vector, while f is applied transverse force per unit area. The director rotation $\boldsymbol{\beta}$ is related to the right-hand-rule rotation vector $\boldsymbol{\theta}$ via an alternating tensor, i.e.

$$\beta_i = e_{ij}\ \theta_j\ ; \quad e_{ij} = \begin{bmatrix} 0 & 1 \\ -1 & 0 \end{bmatrix} \tag{2.21}$$

The variational formulation for the boundary value problem (2.15) to (2.20) is given as *Problem (P)*

$$\Pi(\bar{\boldsymbol{\beta}}, \bar{w}) = \frac{1}{2} \int_\Omega \bar{\beta}_{i,j}\ C^B_{ijkl}\ \bar{\beta}_{k,l}\ d\Omega + \frac{1}{2} \int_\Omega \bar{\gamma}_i\ C^S_{ij}\ \bar{\gamma}_j\ d\Omega - \int_\Omega \bar{w}\ f\ d\Omega \tag{2.22}$$

Variational formulation (2.22) requires that the C^0-continuity be imposed on both rotation $\bar{\boldsymbol{\beta}}$ ($\bar{\boldsymbol{\theta}}$) and the displacement $\bar{w}$ fields. The corresponding variational equation is given as

$$0 = D\Pi(\boldsymbol{\beta}, w) \cdot (\bar{\boldsymbol{\beta}}, \bar{w}) = \int_\Omega \bar{\beta}_{i,j}\ C^B_{ijkl}\ \beta_{k,l}\ d\Omega + \int_\Omega \bar{\gamma}_i\ C^S_{ij}\ \gamma_j\ d\Omega - \int_\Omega \bar{w}\ f\ d\Omega \tag{2.23}$$

The equation (2.23) is chosen as a starting point in discrete approximation for Reissner-Mindlin plate, presented in the next section.

3. FINITE ELEMENT INTERPOLATION

The particular choice for finite dimensional spaces and the resulting discrete variational formulations for both thick shell and solid elements are presented in this section. The superscript h is a mesh parameter which is also used to denote and distinguish the discrete quantities.

3.1. Solid Element

The symmetric tensors in (2.12), in the context of the discrete approximation, are mapped into the corresponding vectors in a standard manner, e.g.

$$symm\, u_{i,j} \rightarrow symm\, \nabla \mathbf{u}^h = \langle u_{1,1}; u_{2,2}; u_{3,3}; u_{1,2}+u_{2,1}; u_{2,3}+u_{3,2}; u_{1,3}+u_{3,1} \rangle^T \tag{3.1}$$

and the skew-symmetric tensors are mapped into their axial vectors, i.e.

$$\psi_{ij} \rightarrow \boldsymbol{\psi}^h = \langle \psi_1; \psi_2; \psi_3 \rangle^T \tag{3.2}$$

and

$$skew\, u_{i,j} \rightarrow skew\, \nabla \mathbf{u}^h = \tfrac{1}{2} \langle u_{3,2}-u_{2,3}; u_{1,3}-u_{3,1}; u_{2,1}-u_{1,2} \rangle^T \tag{3.3}$$

The variational equation which corresponds to the discrete version of *Problem (M)*, *Problem* (M^h) is

$$\begin{aligned} 0 = & \int_{\Omega^e} symm\, \nabla \bar{\mathbf{u}}^{h\,T}\, \mathbf{C}\, symm\, \nabla \mathbf{u}^h \, d\Omega + \int_{\Omega^e} skew\, \bar{\boldsymbol{\sigma}}^{h\,T}\, (skew\, \nabla \mathbf{u}^h - \boldsymbol{\psi}^h)\, d\Omega \\ & + \int_{\Omega^e} (skew\, \nabla \bar{\mathbf{u}}^h - \bar{\boldsymbol{\omega}}^h)^T\, skew\, \boldsymbol{\sigma}^h \, d\Omega \\ & - \gamma^{-1} \int_{\Omega^e} skew\, \bar{\boldsymbol{\sigma}}^{h\,T}\, skew\, \boldsymbol{\sigma}^h \, d\Omega - \int_{\Omega^e} \bar{\mathbf{u}}^{hT}\, \mathbf{f}\, d\Omega \end{aligned} \tag{3.4}$$

We consider an 8-node solid element shown in Figure 1. The reference configuration of the element is defined by the 8-node mapping, i.e.

$$\mathbf{x} = \sum_{I=1}^{8} N_I^e(r,s,t)\, \mathbf{x}_I \tag{3.5}$$

where $\mathbf{x}$ represents global coordinates $(x_1,x_2,x_3)^T$ and $N_I(r,s,t)$ are the isoparametric shape functions (see Zienkiewicz & Taylor [1989])

$$N_I^e(r,s,t) = \frac{1}{8}\,(1+r_I r)\,(1+s_I s)\,(1+t_I t)\,; \quad I=1,2,\ldots,8 \tag{3.6}$$

Natural coordinates (r,s,t) are defined on the interval $\{-1,1\}$. The interpolation for displacements, $\mathbf{u}^h = (u_1,u_2,u_3)^T$, is derived from a 20-node parent element (see Figure 1)

$$\begin{pmatrix} u_1 \\ u_2 \\ u_3 \end{pmatrix} = \mathbf{u}^h = \sum_e \sum_{I=1}^{8} N_I^e(r,s,t)\, \mathbf{u}_I + \sum_e \sum_{I=9}^{20} N_I^e(r,s,t)\, \Delta\mathbf{u}_I \tag{3.7}$$

where $\Delta\mathbf{u}_I$ are hierarchical displacements (relative to the 8-node interpolation values) and

$$N_I^e(r,s,t) = \frac{1}{4}\,(1-r^2)\,(1+s_I s)\,(1+t_I t)\,; \quad I=17,18,19,20 \tag{3.8}$$

$$N_I^e(r,s,t) = \frac{1}{4}\,(1+r_I r)\,(1-s^2)\,(1+t_I t)\,; \quad I=9,11,13,15 \tag{3.9}$$

$$N_I^e(r,s,t) = \frac{1}{4}\,(1+r_I r)\,(1+s_I s)\,(1-t^2)\,; \quad I=10,12,14,16 \tag{3.10}$$

are Serendipity shape functions (see Zienkiewicz & Taylor [1989]) for the mid-edge nodes of the 20-node element.

The tangential hierarchical mid-edge displacements along each edge are set to an average of the corresponding displacement values at the corner nodes, which is consistent with the constraint on linear displacement variation along the element edges. The quadratic variation of the displacement components perpendicular to the element edges is retained. The mid-edge hierarchical displacement components perpendicular to element edges are eliminated by introducing corner node drilling rotations $\boldsymbol{\psi}_I$. The independent rotation field is interpolated in isoparametric fashion as

$$\begin{pmatrix} u_4 \\ u_5 \\ u_6 \end{pmatrix} \equiv \begin{pmatrix} \psi_1 \\ \psi_2 \\ \psi_3 \end{pmatrix} = \boldsymbol{\psi}^h = \sum_e \sum_{I=1}^{8} N_I^e(r,s,t)\, \boldsymbol{\psi}_I \tag{3.11}$$

The resulting element possesses totally 48 degrees of freedom, three displacement components and three rotations at each of the 8 corner nodes. The displacement interpolation is constructed by systematically using the same kind of transformation over each element edge. The introduced constraints can be given directly in global coordinate system (x_1,x_2,x_3), to yield the non-conventional interpolation for the displacement field (see Figure 1)

$$\begin{pmatrix} u_1 \\ u_2 \\ u_3 \end{pmatrix} = \mathbf{u}^h = \sum_e \sum_{I=1}^{8} N_I^e(r,s,t)\,\mathbf{u}_I + \sum_e \sum_{I=9}^{20} N_I^e(r,s,t)\,\frac{l_{JK}}{8}\,[\mathbf{n}_{JK}\,\mathbf{m}_{JK}^T - \mathbf{m}_{JK}\,\mathbf{n}_{JK}^T]\,(\boldsymbol{\psi}_K - \boldsymbol{\psi}_J) \tag{3.12}$$

where l_{JK} is the length of the element edge between the corner nodes J and K, i.e.

$$\mathbf{l}_{JK} = \begin{pmatrix} x_{K1}-x_{J1} \\ x_{K2}-x_{J2} \\ x_{K3}-x_{J3} \end{pmatrix} \; ; \quad l_{JK} = ((x_{K1}-x_{J1})^2+(x_{K2}-x_{J2})^2+(x_{K3}-x_{J3})^2)^{1/2} \tag{3.13}$$

In (3.12) above, the vectors $\mathbf{n}_{JK}$ and $\mathbf{m}_{JK}$ are orthogonal to the element edge JK and mutually orthogonal, i.e.

$$\mathbf{l}_{JK}^T\,\mathbf{m}_{JK} = 0 \; ; \quad \mathbf{l}_{JK}^T\,\mathbf{n}_{JK} = 0 \; ; \quad \mathbf{m}_{JK}^T\,\mathbf{n}_{JK} = 0 \; ; \quad [\mathbf{l}_{JK}\,\mathbf{m}_{JK}\,\mathbf{n}_{JK}] = l_{JK} \tag{3.14}$$

Note that the independent rotation field $\boldsymbol{\psi}$ is continuous across the element boundaries (see (3.11)), which is enforced not by the governing variational equation (3.4) but by the chosen displacement interpolation (3.12).

The skew-symmetric stress field is interpolated independently over each element, i.e.

$$skew\ \boldsymbol{\sigma}^h = \sum_e \mathbf{S}^e\,\boldsymbol{\sigma}_0^e \tag{3.15}$$

The interpolation of the skew-symmetric stress (3.15) is a linear polynomial given in global coordinates $(x_1,x_2,x_3)^T$. Namely, if $\boldsymbol{\sigma}_0^e$ are six skew-symmetric stress interpolation parameters defined at the element level then

$$\mathbf{S}^e = \begin{bmatrix} 1 & x_1 & 0 & 0 & 0 & 0 \\ 0 & 0 & 1 & x_2 & 0 & 0 \\ 0 & 0 & 0 & 0 & 1 & x_3 \end{bmatrix} \tag{3.16}$$

A constant interpolation for the skew-symmetric stress in the membrane problems (see Ibrahimbegovic, Taylor & Wilson [1989]) is consistent with the chosen linear polynomial interpolation for the skew-symmetric stress (3.16); namely, it is recovered as a projection of (3.16) onto the membrane plane.

We further define matrix notation for the infinitesimal strains computation as

$$symm\ \nabla\ \mathbf{u}^e = \mathbf{B}_I^e\,\mathbf{u}_I + \mathbf{G}_I^e\,\boldsymbol{\psi}_I \tag{3.17}$$

where $\mathbf{u}_I$ and $\boldsymbol{\psi}_I$ are nodal values of the displacement and the rotation fields, respectively. The $\mathbf{B}_I^e$ matrix in (3.17) has the standard form

$$\mathbf{B}_I^{eT} = \begin{bmatrix} N^e_{I,x_1} & 0 & 0 & N^e_{I,x_2} & 0 & N^e_{I,x_3} \\ 0 & N^e_{I,x_2} & 0 & N^e_{I,x_1} & N^e_{I,x_3} & 0 \\ 0 & 0 & N^e_{I,x_3} & 0 & N_{I,x_2} & N^e_{I,x_1} \end{bmatrix} \quad ; \qquad I=1,2,..,8 \tag{3.18}$$

and the part of the displacement interpolation associated with the rotation $\boldsymbol{\psi}_I$ defines $\mathbf{G}_I^e$. If we define the transformation matrix for the element edge between corner nodes I and J

$$\mathbf{T}_{IJ} = \frac{l_{IJ}}{8} \left[\mathbf{n}_{IJ}\ \mathbf{m}_{IJ}^T - \mathbf{m}_{IJ}\ \mathbf{n}_{IJ}^T\right] \tag{3.19}$$

then the matrix $\mathbf{G}_I^e$ is obtained by summing over element edges which meet at node I

$$\mathbf{G}_I^e = \sum_{edge} \mathbf{B}_L^e\ \mathbf{T}_{IJ} \tag{3.20}$$

The discrete operator $\mathbf{G}^e$ needs to be modified to avoid element locking tendencies. The modification is discussed in the Appendix I, along with the similar modification performed to avoid shear locking in the thick shell elements.

Furthermore, we denote infinitesimal rotation

$$skew\ \nabla\ \mathbf{u}^e = \mathbf{A}_I^e\ \mathbf{u}_I + \mathbf{F}_I^e\ \boldsymbol{\psi}_I \tag{3.21}$$

and

$$skew\ \nabla\ \mathbf{u}^e - \boldsymbol{\psi}^e = \mathbf{A}_I^e\ \mathbf{u}_I + \left[\mathbf{F}_I^e - N_I^e\,\mathbf{I}\right]\ \boldsymbol{\psi}_I = \mathbf{A}_I^e\ \mathbf{u}_I + \hat{\mathbf{F}}_I^e\ \boldsymbol{\psi}_I \tag{3.22}$$

where

$$\mathbf{A}_I^e = \begin{bmatrix} 0 & -\frac{1}{2} N^e_{I,x_3} & \frac{1}{2} N^e_{I,x_2} \\ \frac{1}{2} N^e_{I,x_3} & 0 & -\frac{1}{2} N^e_{I,x_1} \\ -\frac{1}{2} N^e_{I,x_2} & \frac{1}{2} N^e_{I,x_1} & 0 \end{bmatrix}, \quad I=1,2,..,8 \tag{3.23}$$

and $\mathbf{F}_I^e$ can be obtained by systematic transformations performed over each element edge which meet at node I

$$\mathbf{F}_I^e = \sum_{edge} \mathbf{A}_L^e \, \mathbf{T}_{IJ} \tag{3.24}$$

The first term in the discrete formulation (3.4) of *Problem* (M^h) gives rise to the element stiffness matrix

$$\mathbf{K}^e = \int_{\Omega^e} \left[\mathbf{B}^e \, \mathbf{G}^e\right]^T \mathbf{C} \left[\mathbf{B}^e \, \mathbf{G}^e\right] d\Omega \tag{3.25}$$

The second term in (3.4) is denoted as

$$\mathbf{H}^{eT} = \int_{\Omega^e} \mathbf{S}^{eT} \left[\mathbf{A}^e \, \hat{\mathbf{F}}^e\right] d\Omega \tag{3.26}$$

and the last term in (3.4) defines

$$\mathbf{M}^e = \gamma^{-1} \int_{\Omega^e} \mathbf{S}^{eT} \, \mathbf{S}^e \, d\Omega \tag{3.27}$$

With this notation at hand, the discrete mixed-type variational formulation (3.4) for one element can be rewritten as

$$\begin{bmatrix} \mathbf{K}^e & \mathbf{H}^e \\ \mathbf{H}^{eT} & -\mathbf{M}^e \end{bmatrix} \begin{pmatrix} \mathbf{a} \\ \boldsymbol{\sigma}_0^e \end{pmatrix} = \begin{pmatrix} \mathbf{f} \\ \mathbf{0} \end{pmatrix} \quad ; \quad \mathbf{a} = \begin{pmatrix} \mathbf{u} \\ \boldsymbol{\psi} \end{pmatrix} \tag{3.28}$$

Since the skew-symmetric part of the stress is interpolated independently in each element, the corresponding part of the stiffness matrix in (3.28) may be eliminated at the element level using static condensation (see Wilson [1974]) to yield

$$\hat{\mathbf{K}}^e \, \mathbf{a} = \mathbf{f} \quad ; \quad \hat{\mathbf{K}}^e = \mathbf{K}^e + \mathbf{H}^e \, \mathbf{M}^{e\,-1} \, \mathbf{H}^{eT} \tag{3.29}$$

where inversion of $\mathbf{M}^e$ can be given in a closed form by inverting 2×2 submatrices on the diagonal (follows from (3.16) and (3.27)).

In a completely analogous manner we can construct an approximation for the displacement-type variational formulation. The discrete version of *Problem (D)* follows from (2.14) as *Problem* (D^h)

$$0 = \int_{\Omega^e} symm\, \nabla \bar{\mathbf{u}}^{h\,T}\, \mathbf{C}\, symm\, \nabla \mathbf{u}^h \, d\Omega$$

$$+ \gamma \int_{\Omega^e} (skew\, \nabla\, \bar{\mathbf{u}}^h - \bar{\boldsymbol{\psi}}^h)^T\, (skew\, \nabla\, \mathbf{u}^h - \boldsymbol{\psi}^h)\, d\Omega - \int_{\Omega^e} \bar{\mathbf{u}}^{h\,T}\, \mathbf{f}\, d\Omega \tag{3.30}$$

The rotation and displacement fields are again interpolated by (3.11) and (3.12), respectively. The first term in the displacement-type formulation (3.30) produces the same element stiffness matrix $\mathbf{K}^e$ defined by (3.25). The second term in (3.30), however, is different. Note that using the interpolations for displacement (3.12) and rotation (3.11), this term can be directly obtained via (3.22)

$$\mathbf{P}^e = \gamma \int_{\Omega^e} \left[\mathbf{A}^e\, \hat{\mathbf{F}}^e\right]^T \left[\mathbf{A}^e\, \hat{\mathbf{F}}^e\right] d\Omega \tag{3.31}$$

Hence the matrix counterpart of (3.30) for one element in a displacement-type formulation is

$$\left[\mathbf{K}^e + \mathbf{P}^e\right] \mathbf{a} = \mathbf{f} \;; \quad \mathbf{a} = \begin{pmatrix} \mathbf{u} \\ \boldsymbol{\psi} \end{pmatrix} \tag{3.32}$$

The parts of the element stiffness matrix $\mathbf{K}^e$ and $\mathbf{H}^e$ in (3.27) and (3.32) are computed using a 14-point quadrature, given by Irons [1971]. The matrix $\mathbf{P}^e$ in (3.32) is integrated by 2×2×2 Gaussian quadrature. By fully integrating $\mathbf{K}^e$ and combining with $\mathbf{P}^e$ or $\mathbf{H}^e\mathbf{M}^{e\,-1}\mathbf{H}^{eT}$ the spurious zero energy modes are prevented. The 'equivalence theorem' of Malkus & Hughes [1978] indicates that this approach of selective reduced integration (3.32) is not equivalent to the mixed formulation (3.29). Namely, six parameters for $skew\boldsymbol{\sigma}$ are used in the mixed-type formulation versus 8-point integration rule on the penalty term in displacement-type formulation. However, for the regular meshes the performances of the solid elements based on two formulations are quite similar.

3.2. Thick Shell Element

The underlying interpolation field for thick shell element is very similar to the one used for the solid element. However, the motivation and the starting variational formulation is different.

The discretized version of the variational formulation for thick plate *Problem P* is given as *Problem* (P^h)

$$0 = \int_{\Omega^e} symm\,\nabla \bar{\boldsymbol{\beta}}^{hT}\, \mathbf{C}^B\, symm\nabla \boldsymbol{\beta}^h\, d\Omega + \int_{\Omega^e} \bar{\boldsymbol{\gamma}}^{hT}\, \mathbf{C}^S\, \boldsymbol{\gamma}^h\, d\Omega - \int_{\Omega^e} \bar{w}^h\, f\, d\Omega \quad (3.33)$$

In (3.33) above, we mapped the tensors in (2.23) into the corresponding matrix quantities, e.g.

$$\beta_{i,j} \rightarrow symm\,\nabla \boldsymbol{\beta}^h = <\beta_{1,1}\ ;\ \beta_{2,2}\ ;\ \beta_{1,2}+\beta_{2,1}> \quad (3.34)$$

$$\gamma_i \rightarrow \boldsymbol{\gamma}^h = <\gamma_1\ ;\ \gamma_2> \quad (3.35)$$

We next consider the finite element interpolation field for the discretization of the thick plate variational formulation (3.33). For motivation, we first consider a Timoshenko beam in which shear deformations are included (see Taylor [1987]). The strain displacement relations are given by

$$\kappa = \frac{d\theta}{dx} \quad (3.36)$$

and

$$\gamma = \frac{dw}{dx} + \theta \quad (3.37)$$

which can be recovered as a subset of adequate thick plate formulation (2.15) and (2.16).

We use isoparametric interpolation to define the geometry and the rotation fields

$$x = N_1^e(r)\, x_1 + N_2^e(r)\, x_2 \quad (3.38)$$

$$\theta = N_1^e(r)\, \theta_1 + N_2^e(r)\, \theta_2 \quad (3.39)$$

and hierarchical quadratic interpolation to define the transverse displacements

$$w = N_1^e(r)\, w_1 + N_2^e(r)\, w_2 + N_3^e(r)\, \Delta w_3 \quad (3.40)$$

with the shape functions given as

$$N_1^e(r) = \frac{1}{2}\,(1-r)\ ;\quad N_2^e(r) = \frac{1}{2}\,(1+r)\ ;\quad N_3^e(r) = \frac{1}{2}\,(1-r^2) \quad (3.41)$$

Within the context of discrete approximation, the strains are defined by substituting (3.39) and (3.40) into the (3.36) and (3.37) to get

$$\kappa = \frac{1}{l}\,(\theta_2 - \theta_1)\ ;\quad l = x_2 - x_1 \quad (3.42)$$

and

$$\gamma = \frac{1}{l}(w_2 - w_1) + \frac{1}{2}(\theta_1 + \theta_2) + r\left[\frac{1}{2}(\theta_2 - \theta_1) - \frac{4}{l}\Delta w_3\right] \tag{3.43}$$

If the relative nodal displacement Δw_3 is set to zero then all fields are approximated by linear interpolation. In that case, the linear varying term in shear is directly related to the change of curvature, i.e. it is not possible to have a constant shear strain in the presence of bending behavior. When thin beams with negligible 'constant' shear strains are analyzed, this inconsistency is reflected by 'shear locking' phenomena. The locking phenomena of this kind may be avoided by constraining to zero the term in brackets in (3.43). This yields interpolation for the displacement in the form

$$w = N_1^e(r)\, w_1 + N_2^e(r)\, w_2 + \frac{l}{8} N_3^e(r)\,(\theta_2 - \theta_1) \tag{3.44}$$

An alternative interpretation of the similar interpolation field for thick shell elements is that 'Kirchhoff modes' must be attainable in underlying interpolation (see Tessler & Hughes [1983]). The plate elements which explicitly enforce discrete Kirchhoff constraints are able to obtain the higher order interpolation (see Batoz et al. [1980] or Batoz & Tahar [1982]). For the same order of interpolation, the plate elements based on Reissner-Mindlin theory need extra degrees of freedom (e.g., see Brezzi et al. [1989] or Zienkiewicz et al. [1989]).

In the context of thick plates and shells, the interpolation field equivalent to (3.44) needs to be corrected to avoid the shear locking. This is discussed in the Appendix I. The resulting element performs much better than the similar one considered earlier by Tessler & Hughes [1983] without the need of introducing numerically adjusted parameters or residual bending flexibility (see MacNeal [1978]).

We further consider a 4-node quadrilateral element shown in Figure 2. The reference surface of the element is defined by

$$\mathbf{x} = \sum_{I=1}^{4} N_I^e(r,s)\, \mathbf{x}_I \tag{3.45}$$

where $\mathbf{x}$ now represents the local coordinates $(x_1,x_2)^T$ and $N_I(r,s)$ are the isoparametric shape functions (Zienkiewicz & Taylor [1989])

$$N_I^e(r,s) = \frac{1}{4}(1+r_I r)(1+s_I s)\,; \quad I=1,2,3,4 \tag{3.46}$$

Natural coordinates (r,s) are defined on the interval $\{-1,1\}$. The interpolation for in-plane rotations is

$$\begin{pmatrix}\theta_1\\ \theta_2\end{pmatrix} = \boldsymbol{\theta}^h = \sum_e \sum_{I=1}^{4} N_I^e(r,s)\ \boldsymbol{\theta}_I \tag{3.47}$$

and transverse displacement interpolation is obtained by generalizing the simple beam interpolation

$$w^h = \sum_e \sum_{I=1}^{4} N_I^e(r,s)\ w_I - \sum_e \sum_{I=5}^{8} N_I^e(r,s)\ \frac{l_{JK}}{8}\ \mathbf{n}_{JK}^T\ (\boldsymbol{\theta}_K - \boldsymbol{\theta}_J) \tag{3.48}$$

where

$$N_I^e(r,s) = \frac{1}{2}\ (1-r^2)\ (1+s_I s)\ ; \quad I=5,7 \tag{3.49}$$

$$N_I^e(r,s) = \frac{1}{2}\ (1+r_I r)\ (1-s^2)\ ; \quad I=6,8 \tag{3.50}$$

are Serendipity shape functions (see Zienkiewicz & Taylor [1989]) for the mid-sides of the 8-node element. In (3.48), l_{JK} and $\mathbf{n}_{JK}$ are the length and the outward unit normal vector on the element side associated with the corner nodes J and K, i.e.

$$\mathbf{n}_{JK} = \begin{pmatrix} n_1\\ n_2\end{pmatrix} = \begin{pmatrix}\cos\alpha_{JK}\\ \sin\alpha_{JK}\end{pmatrix} \qquad l_{JK} = ((x_{K1}-x_{J1})^2+(x_{K2}-x_{J2})^2)^{1/2} \tag{3.51}$$

and FORTRAN-like definition of adjacent corner nodes

$$J = I-4\ ; \quad K = mod(I,4)+1 \tag{3.52}$$

Note that the finite element displacement interpolation for thick shell element (3.48) may be directly recovered from the solid element interpolation (3.12).

We further define matrix notation for curvature vector

$$symm\ \nabla\ \boldsymbol{\beta}^e = \mathbf{B}_I^e\ \boldsymbol{\beta}_I = \mathbf{B}_I^e\ \mathbf{e}\ \boldsymbol{\theta}_I \tag{3.53}$$

where $\boldsymbol{\theta}_I$ are nodal values of the rotation fields and $\mathbf{e}$ is the alternating matrix defined in (2.21). The $\mathbf{B}_I^e$ matrix in (3.53) has the standard form

$$\mathbf{B}_I^{eT} = \begin{bmatrix} N_{I,x_1}^e & 0 & N_{I,x_2}^e\\ 0 & N_{I,x_2}^e & N_{I,x_1}^e\end{bmatrix}\ ; \qquad I=1,2,3,4 \tag{3.54}$$

Furthermore, we denote shear strain interpolation as

$$\boldsymbol{\gamma}^e = \mathbf{b}_I^{eT} w_I + \mathbf{G}_I^e \boldsymbol{\theta}_I \tag{3.55}$$

where

$$\mathbf{b}_I^e = < N_{I,x_1}^e \; ; \; N_{I,x_2}^e > \quad , \quad I=1,2,3,4 \tag{3.56}$$

and

$$\mathbf{G}_I^e = \begin{bmatrix} -\frac{1}{8}(l_{IJ} \cos \alpha_{IJ} \, NS_{L,x_1}^e - l_{IK} \cos \alpha_{IK} \, NS_{M,x_1}^e) & N_I - \frac{1}{8}(l_{IJ} \sin \alpha_{IJ} \, NS_{L,x_1}^e - l_{IK} \sin \alpha_{IK} \, NS_{M,x_1}^e) \\ -N_I - \frac{1}{8}(l_{IJ} \cos \alpha_{IJ} \, NS_{L,x_2}^e - l_{IK} \cos \alpha_{IK} \, NS_{M,x_2}^e) & -\frac{1}{8}(l_{IJ} \sin \alpha_{IJ} \, NS_{L,x_2}^e - l_{IK} \sin \alpha_{IK} \, NS_{M,x_2}^e) \end{bmatrix} \tag{3.57}$$

where, in (3.57) above

$$I=1,2,3,4 \; ; \; M = I + 4 \; ; \; L = M - 1 + 4 \, aint(1/I) \; ; \; K = mod(M,4) + 1 \; ; \; J = L - 4 \tag{3.58}$$

The discrete formulation (3.33) of *Problem* (P^h) gives rise to the thick plate element stiffness matrix

$$\mathbf{K}^e = \int_{\Omega^e} \mathbf{B}^{eT} \, \mathbf{C}^B \, \mathbf{B}^e \, d\Omega + \int_{\Omega^e} \left[\mathbf{b}^{eT} \, \mathbf{G}^e \right]^T \mathbf{C}^S \left[\mathbf{b}^{eT} \, \mathbf{G}^e \right] d\Omega \tag{3.59}$$

4. NUMERICAL EVALUATION

The performance of both finite elements presented herein, the thick shell and the solid, is evaluated on a set of examples presented in this section. Both elements can be used in analysis of thick shells and plates. The solid element, in addition, can be used in a general three-dimensional problems. The most important value of it, most probably, is in providing a consistent combination with beam and shell elements with rotational degrees of freedom. All the numerical results reported in foregoing are obtained with the computer program *SAP* (see Wilson [1980]).

4.1. Solid Element

4.1.1. The Patch Test

The solid element patch test (see Taylor et al. [1986]) is performed on both a single element with a minimum number of constraints (see Figure 3) and a patch of solid elements given in a standard problem set of MacNeal & Harder [1985]. Both mixed-type and

displacement-type elements pass the patch tests. In the results to follow, these elements are denoted M-type and D-type, respectively.

4.1.2. A Simple Beam: The Higher Order Patch Test

A simple beam with a length to height aspect ratio of 10 is subjected to a pure bending state. The beam is modeled by one row of six solid elements with rotational degrees of freedom as shown in Figure 4. Only a minimum number of restraints is imposed, leaving all the rotational degrees of freedom free. Two load cases are considered. The first load case is a unit couple applied at both ends and represents a higher-order patch test (see Taylor et al. [1986]). When a regular mesh is used, the solution is exact. For a distorted mesh (see Figure 4) the accuracy is still good. The second load case is, to our knowledge, a novel test. The loading is again a unit moment, but this time applied as a concentrated moment at the drilling degrees of freedom at both ends. The difference from the exact solution, for regular mesh, is due to the fact that a single concentrated moment at a drilling degree of freedom is not a consistent loading (which follows from displacement interpolation (3.12)). The results of the analysis (see Table 1) can be compared with the beam theory exact solution of 1.5 for vertical displacement and 0.6 for end rotation.

The value of parameter γ is set of the order of shear modulus. The results are more sensitive to the choice of γ than in the membrane case (see Ibrahimbegovic, Taylor & Wilson [1989]).

Table 1. A Simple Beam (Fig. 4)

Formulation	Mesh	Load Case	Vert. Displ.	End Rot.
M-type	reg.	1	1.5	0.6
M-type	dist.	1	1.3227	0.56759
M-type	reg.	2	1.5	0.62983
M-type	dist.	2	1.3276	0.65514
D-type	reg.	1	1.5	0.6
D-type	dist.	1	1.2719	0.52819
D-type	reg.	2	1.5	0.64450
D-type	dist.	2	1.2800	0.62464
beam theory	-	1 or 2	1.5	0.6

4.1.3. A Cantilever Beam

A shear-loaded cantilever beam is selected as a test problem by many authors (e.g., see Bergan & Fellipa [1985], Allman[1988], MacNeal & Harder [1988], Hughes et al.

[1989], Pian & Sumihara [1984]). The elasticity solution (e.g., see Timoshenko & Goodier [1951] and Hughes [1987]) for the tip displacement is

$$u_2 = \frac{Pl^3}{3EI} + \frac{(4+5\nu)Pl}{2Ehb} = 102.625$$

for $b = h$ and the properties selected (see Figure 5 for details).

The finite element solution is obtained for two coarse regular meshes of two and four elements. The equivalent results are also obtained by using the thick shell elements presented herein, denoted as Th. Shell. All are presented in Table 2.

Table 2. Tip Displ. of Short Cantilever Beam (Fig. 5)			
Mesh	M-type	D-type	Th. Shell
2×1	89.129	88.990	96.429
4×1	102.301	101.292	101.328
elast. sol.	102.625	102.625	102.625

4.1.4. Simply Supported Square Plate

We also consider the performance of the solid element of this kind in the analysis of simply supported square plate under uniform loading q (see Figure 6). Due to the symmetry, only one quarter of the plate is modeled imposing the appropriate boundary conditions. So called hard boundary conditions are imposed on the simple supports. The results of the analysis are given in Table 3. They can be compared with the series solutions also presented in Table 3. For thick plate (t=1), the performance of the elements is quite satisfying. In the thin plate case (t=0.1), both solid elements exhibit a moderate shear locking, with M-type element being slightly superior.

Table 3. Center Displ. of Simply Supp. Square Plate (Fig. 6)				
	Thick plate (t=1)		Thin plate (t=0.1)	
Mesh	M-type	D-type	M-type	D-type
2×2	40.980	40.232	23713	23123
4×4	42.149	42.138	32768	31782
series sol.	42.728	42.728	40644	40644

4.2. Thick Shell Element

4.2.1. The Patch Test

The patch test (see Taylor et al. [1986]) is performed on a single element test for a uniform bending, as well as on the patch of plate elements given in a problem set of Mac-Neal & Harder [1985]. All tests are successfully passed.

4.2.2. Simply Supported Square Plate

We again consider the simply supported square plate under uniform loading q (see Figure 6). The analysis is performed on the model which uses only one quarter of the plate, but for the more refined regular meshes (see Figure 7). The results of the analysis are given in Table 4. For comparison, the results obtained with $T1$ four-node plate element of Hughes & Tezduyar [1981] are also presented. The $T1$ plate element is identical to *MITC*4 plate element of Bathe & Dvorkin [1985] and of very similar performance as incompatible modes based plate element of Simo & Rifai [1989]. The performance of our element (denoted as *Th. Shell* in Table 4) is quite satisfying for both thick and thin plates, i.e. no shear locking occurs in the thin plate case. Moreover, our element performance is fully equivalent to $T1$ class of plate elements, and the formulation is somewhat simpler.

Table 4. Center Displ. of Simply Supp. Square Plate (Fig. 6)

	Thick plate (t=1)		Thin plate (t=0.1)	
Mesh	Th. Shell	T1	Th. Shell	T1
2×2	41.899	41.902	39463	39712
4×4	42.545	42.545	40421	40436
8×8	42.684	42.684	40592	40593
16×16	42.717	42.717	40632	40632
series sol.	42.728	42.728	40664	40664

4.2.3. Simply Supported Circular Plate

The circular plate example is selected to demonstrate the performance of the thick shell element presented herein in distorted configuration. The mechanical properties of the plate are the same like for the square plate in Figure 6 and the radius R=5. Due to symmetry, only one quadrant of the circular plate has been discretized with four finite element meshes. A typical finite element model for 8×8 mesh is presented in Figure 8. The analytical solution is given as

$$w(0) = \frac{q\ a^4}{64\ E\ (1-\nu^2)/12}\left(\frac{5+\nu}{1+\nu} + \frac{8}{3\,c\,(1-\nu)}\left(\frac{t}{a}\right)^2\right)$$

where c is a shear correction factor (taken 5/6 when computing all the results presented herein). The performance of the element is quite satisfying in both the thin and thick plate analysis (see Table 5).

Table 5.	Center Displ. of Simply Supp. Circ. Plate (Fig. 8)	
Mesh	Thick plate (t=1)	Thin plate (t=0.1)
2×2	37.38190	33856
4×4	40.58131	38696
8×8	41.346613	39574
16×16	41.53630	39768
series sol.	41.59942	39831

4.2.4. *Hemispherical Shell with 18°* Hole

The performance of the shell element is also evaluated on a standard test problem of a hemispherical shell with a hole (see MacNeal & Harder [1985]), presented in Figure 9. It is important to establish that the proposed formulation causes no membrane locking when applied to shell analysis. The results for the maximum displacement obtained with refined finite element meshes (Figure 10) are given in Table 6. The results of this analysis should be compared with the solution of 0.094 given by MacNeal & Harder [1985] and the new value 0.093 suggested recently by Simo et al. [1989]. When the mesh is refined, the convergence to the exact solution can be observed.

Table 6.	Hemispherical Shell (Fig. 9)
Mesh	Maximum Displacement
8×8	0.088768
12×12	0.092487
16×16	0.092982
series sol.	0.093

5. CLOSURE

We have presented the solid elements with rotational degrees of freedom, i.e. for an 8-node brick element 48 degrees of freedom are present. Elements are derived from the variational principles employing independent rotational fields, which is in contrast with the free-formulation based elements. Mixed variational formulation which employs skew-

symmetric stress and penalty variational formulation where skew-symmetric stress is eliminated are both used to derive the corresponding discrete approximations. Special hierarchical interpolation is employed in the process. The mixed and penalty formulations are not equivalent (in the sense of Malkus & Hughes [1978]), but exhibit similar performances, with the mixed formulation being slightly advantageous. In terms of accuracy and the computational efforts involved, the solid elements of this kind are in-between the classical 8-node brick and 27-node Lagrangian elements. However, their most important value is in providing a unified approach to modeling of complex structures where other kinds of elements with rotational degrees of freedom appear as well.

In addition, a novel 4-node thick shell element with six degrees of freedom per node, is formed by superposing previously discussed membrane elements with drilling degrees of freedom (see Ibrahimbegovic, Taylor & Wilson [1989]) and the thick plate elements based on Reissner-Mindlin plate theory. In the plate analysis problems, the element performance is fully equivalent to other 4-node elements (e.g. $T1$ of Hughes & Tezduyar [1981] or $MITC4$ of Bathe & Dvorkin [1985]), but its formulation is simpler. The crucial step in providing a good element performance in thin plate analysis is in shear locking correction which is discussed in the Appendix I along with the similar correction performed on solid elements. In the shell analysis problems, the element is free of membrane locking.

We have evaluated performance of the elements only in the context of linear quasi-static problems. However, since the interpolation is provided for all the variables in the formulation, the extension to transient as well as nonlinear problems is straightforward.

ACKNOWLEDGMENT

We wish to thank Professor R.L. Taylor for helpful discussions.

6. APPENDIX I: SHEAR/MEMBRANE LOCKING CORRECTION

The non-conventional interpolations for both the thick shell and solid elements presented herein need to be corrected to avoid the tendencies of locking behavior. The procedure used for that purpose fits into the framework of well-known $B-bar$ methods (see Hughes [1980,87], Simo et al. [1985] or Simo & Hughes [1986]), which arise in formulation for enforcing incompressibility constraint. In our case, the constant strain constraint must be enforced for the contribution of rotational degrees of freedom in hierarchical

displacement interpolation. For solid elements, the constant strain states also ensures the satisfaction of the patch test (see Taylor et al. [1986]). In the membrane part of thick shell elements, similar correction precludes membrane locking when the modeling of shell geometry by the flat elements produces the kinks in the finite element model (see Jetteur & Frey [1986] or Taylor [1987]). For the thick plate, the correction of this kind is crucial in avoiding shear locking phenomena.

I.1. Solid Elements

We want to enforce the possibility of the constant strain state $\boldsymbol{\varepsilon}_c^e$ in the expression for infinitesimal strain. Accordingly, we rewrite (3.17) as

$$symm\ \nabla\ \mathbf{u}^e = \mathbf{B}_I^e\ \mathbf{u}_I + \mathbf{G}_I^e\ \boldsymbol{\psi}_I + \boldsymbol{\varepsilon}_c^e \tag{I.1}$$

Since conventional interpolation is used to approximate nodal displacements contribution to infinitesimal strains, this part can assume arbitrary value, including zero. For that case, we impose the constraint that the remaining part be zero as well, i.e.

$$\mathbf{G}_I^e\ \boldsymbol{\psi}_I + \boldsymbol{\varepsilon}_c^e = \mathbf{0} \tag{I.2}$$

In the variational formulation this constraint is imposed in the weak sense, by augmenting the variational formulation with

$$\sum_e \int_{\Omega^e} \bar{\boldsymbol{\sigma}}_c^e\ (\mathbf{G}_I^e\ \bar{\boldsymbol{\psi}}_I + \bar{\boldsymbol{\varepsilon}}_c^e)\ d\Omega \tag{I.3}$$

where each term is defined independently over each element. In (I.3), $\bar{\boldsymbol{\sigma}}_c^e$ is energy-conjugate to $\bar{\boldsymbol{\varepsilon}}_c^e$. The corresponding variational equation is than obtained as

$$\int_{\Omega^e} \mathbf{G}_I^e\ d\Omega\ \boldsymbol{\psi}_I + \Omega^e\ \boldsymbol{\varepsilon}_c^e = 0 \tag{I.4}$$

from which

$$\boldsymbol{\varepsilon}_c^e = -\frac{1}{\Omega^e} \int_{\Omega^e} \mathbf{G}_I^e\ d\Omega\ \boldsymbol{\psi}_I \tag{I.5}$$

After substituting (I.5) into the (I.1), we recover

$$symm\ \nabla\ \mathbf{u}^e = \mathbf{B}_I^e\ \mathbf{u}_I + \bar{\mathbf{G}}_I^e\ \boldsymbol{\psi}_I \tag{I.6}$$

where

$$\bar{\mathbf{G}}_I^e = \mathbf{G}_I^e - \frac{1}{\Omega^e} \int_{\Omega^e} \mathbf{G}_I^e \, d\Omega \tag{I.7}$$

I.2. Thick Shell Element

For the membrane part of thick shell element, the same kind of correction as given in (I.7) is performed. For the thick plate part, the shear locking correction is performed by utilizing the same kinds of arguments as for the solid element given in the Section I.1. In this case, however, we want to obtain constant (zero) shear strain, which reflects the tendencies in the thin plate limit and alleviates the shear locking. For that reason, the shear strain computation (3.55) is rewritten as

$$\boldsymbol{\gamma}^e = \mathbf{b}_I^{eT} w_I + \mathbf{G}_I^e \, \boldsymbol{\theta}_I + \boldsymbol{\gamma}_c^e \tag{I.8}$$

where $\boldsymbol{\gamma}_c^e$ is interpolated as constant over each element. The shear strains computed from the conventional displacement interpolation can assume arbitrary constant value, including zero. The constraint that the remaining part of (I.8) be zero is

$$\mathbf{G}_I^e \, \boldsymbol{\theta}_I + \boldsymbol{\gamma}_c^e = \mathbf{0} \tag{I.9}$$

The variational formulation of thick plate problem is now augmented with

$$\sum_e \int_{\Omega^e} \bar{\boldsymbol{\tau}}_c^e \, (\mathbf{G}_I^e \, \bar{\boldsymbol{\theta}}_I + \bar{\boldsymbol{\gamma}}_c^e) \, d\Omega \tag{I.10}$$

which has the corresponding variational equation given as

$$\int_{\Omega^e} \mathbf{G}_I^e \, d\Omega \, \boldsymbol{\theta}_I + \Omega^e \, \boldsymbol{\gamma}_c^e = \mathbf{0} \tag{I.11}$$

and the solution for $\boldsymbol{\gamma}_c^e$

$$\boldsymbol{\gamma}_c^e = -\frac{1}{\Omega^e} \int_{\Omega^e} \mathbf{G}_I^e \, d\Omega \, \boldsymbol{\theta}_I \tag{I.12}$$

The modified expression for the shear strain computation is then given as

$$\boldsymbol{\gamma}^e = \mathbf{b}_I^{eT} w_I + \bar{\mathbf{G}}_I^e \, \boldsymbol{\theta}_I \tag{I.13}$$

where

$$\bar{G}_I^e = G_I^e - \frac{1}{\Omega^e} \int_{\Omega^e} G_I^e \, d\Omega \tag{I.14}$$

Note that the shear locking correction (I.14) leaves the interpolation (3.44) for the simple Timeshenko beam unaffected. In the thick plate case, however, the shear correction (I.14) plays the crucial role in alleviating shear locking. Both $\bar{G}$ corrections, (I.7) and (I.14), are performed by utilizing the corrected Serendipity shape functions in the expressions (3.17) and (3.55), respectively, which minimizes the computational efforts involved.

7. REFERENCES

Allman D.J. [1984], A Compatible Triangular Element Including Vertex Rotations for Plane Elasticity Problems, Comput. Struct., 19, 1-8

Allman D.J. [1987], The Constant Strain Triangle with Drilling Rotations: A Simple Prospect for Shell Analysis, Proceedings *The Mathematics of Finite Elements and Applications*, (ed. J.R. Whiteman), Academic Press, 230-236

Allman D.J. [1988], A Quadrilateral Finite Element Including Vertex Rotations for Plane Elasticity Problems, Int. J. Numer. Methods Eng., 26, 717-739

Bathe K.J. [1982], *The Finite Element Procedures in Engineering Analysis*, Prentice-Hall

Bathe K.J. and E.N. Dvorkin [1985], A Four-Node Plate Bending Element Based on Mindlin-Reissner Plate Theory and a Mixed Interpolation, Int. J. Numer. Methods Eng., 21, 367-383

Batoz J.L., K.J. Bathe and L.W. Ho [1980], A Study of Three-Node Triangular Plate Bending Elements, Int. J. Numer. Methods Eng., 15, 1771-1812

Batoz J.L. and M.B. Tahar [1982], Evaluation of a New Quadrilateral Thin Plate Bending Element, Int. J. Numer. Methods Eng., 18, 1655-1677

Bergan P.G. and C.A. Fellipa [1985], A Triangular Membrane Element with Rotational Degrees of Freedom, Comput. Methods Appl. Mech., 50, 25-60

Brezzi F., K.J. Bathe and M. Fortin [1989], Mixed-Interpolated Elements for Reissner-Mindlin Plates, Int. J. Numer. Methods Eng., 28, 1787-1801

Carpenter N., H. Stolarski and T. Belytschko [1985], A Flat Triangular Shell Element with Improved Membrane Interpolation, Commun. Appl. Numer. Methods, 1, 161-168

Hughes T.J.R. [1980], Generalization of Selective Integration Procedures to Anisotropic and Nonlinear Media, Int. J. Numer. Methods Eng., 22, 1413-1418

Hughes T.J.R. and T.E. Tezduyar [1981], Finite Elements Based Upon Mindlin Plate Theory with Particular Reference to the Four-Node Bilinear Isoparametric Element, J. Appl. Mech., 46, 587-596

Hughes T.J.R. [1987], *The Finite Element Method: Linear Static and Dynamic Analysis*, Prentice-Hall

Hughes T.J.R. and F. Brezzi [1989], On Drilling Degrees of Freedom, Comput. Methods Appl. Mech. Eng., 72, 105-121

Hughes T.J.R., F. Brezzi, A. Masud and I. Harari [1989], Finite Element with Drilling Degrees of Freedom: Theory and Numerical Evaluation, preprint

Ibrahimbegovic A., R.L. Taylor and E.L. Wilson [1989], A Robust Membrane Quadrilateral Element With Drilling Degrees of Freedom, Int. J. Numer. Methods Eng.

Ibrahimbegovic A. and E.L. Wilson [1989], A Unified Formulation for Triangular and Quadrilateral Flat Shell Finite Elements With Drilling Degrees of Freedom, Commun. Appl. Numer. Methods

Irons B.M. [1971], Quadrature Rules for Brick Based Finite Elements, Int. J. Numer. Methods Eng., 3, 293-294

Jetteur P. and F. Frey [1986], A Four Node Marguerre Element for Nonlinear Shell Analysis, Eng. Comput., 3, 276-282

MacNeal R.H. [1978], A Simple Quadrilateral Shell Element, Comput. Struct., 8, 175-183

MacNeal R.H. and R.L. Harder [1985], A Proposed Standard Set of Problems to Test Finite Element Accuracy, J. Finite Elem. Anal. Design, 1, 3-20

MacNeal R.H. and R.L. Harder [1988], A Refined Four-Noded Membrane Element with Rotational Degrees of Freedom, Comput. Struct., 18, 75-84

Malkus D.S. and T.J.R. Hughes [1978], Mixed Finite Element Methods - Reduced and Selective Integration Techniques: A Unification of Concepts, Comput. Methods Appl. Mech. Eng., 15, 68-81

Mindlin R.D. [1951], Influence of Rotatory Inertia and Shear in Flexural Motion of Isotropic Elastic Plates, J. Appl. Mech., 18, 31-38

Pian T.H.H. and R. Sumihara [1984], Rational Approach for Assumed Stress Finite Elements, Int. J. Numer. Methods Eng., 20, 1685-1695

Reissner E. [1945], The Effect of Transverse Shear Deformation on the Bending of Elastic Plates, J. Appl. Mech., 12, 69-76

Reissner E. [1965], A Note on Variational Principles in Elasticity, Int. J. Solids Struct., 1, 93-95

Simo J.C., R.L. Taylor and K.S. Pister [1985], Variational and Projection Methods for the Volume Constraint in Finite Deformation Elasto-Plasticity, Comput. Methods Appl. Mech. Eng., 51, 177-208

Simo J.C. and T.J.R. Hughes [1986], On the Variational Foundations of Assumed Strain Method, J. Appl. Mech., 53, 51-54

Simo J.C., D.D. Fox and M.S. Rifai [1989], On a Stress Resultant Geometrically Exact Shell Model Part II: The Linear Theory; Computational Aspects, Comput. Methods Appl. Mech. Eng., 73, 53-92

Simo J.C. and M.S. Rifai [1989], A Class of Mixed Assumed Strain Methods and the Method of Incompatible Modes, preprint

Taylor R.L. and J.C. Simo [1985], Bending and Membrane Elements for Analysis of Thick and Thin Shells, Proceedings NUMETA 85 (eds. J.Middelton and G.N. Pande), 587-591,

Taylor R.L., J.C. Simo, O.C. Zienkiewicz and A.C. Chan [1986], The Patch Test: A Condition for Assessing Finite Element Convergence, Int. J. Numer. Methods Eng., 22, 39-62

Taylor R.L. [1987], Finite Element Analysis of Linear Shell Problems, Proceedings *The Mathematics of Finite Elements and Applications*, (ed. J.R. Whiteman), Academic Press, 211-223

Tessler A. and T.J.R. Hughes [1983], An Improved Treatment of Transverse Shear in the Mindlin-Type Four-Node Quadrilateral Element, Comput. Methods Appl. Mech. Eng., 39, 311-335

Timoshenko S. and J.N. Goodier [1951], *Theory of Elasticity*, McGraw-Hill

Wilson E.L. [1974], The Static Condensation Algorithm, Int. J. Numer. Methods Eng., 8, 199-203

Wilson E.L. [1980], SAP80 - Structural Analysis Program for Small or Large Computer Systems, Proceedings CEPA Fall Conference

Zienkiewicz O.C. and R.L. Taylor [1989], *The Finite Element Method: Basic Formulation and Linear Problems*, vol I, McGraw-Hill

Zienkiewicz O.C., R.L. Taylor, P. Papadopoulos and E. Onate [1989], Plate Bending Elements with Discrete Constraints: New Triangular Elements, Report UCB/SEMM 89/07, University of California, Berkeley

8. LIST OF FIGURES

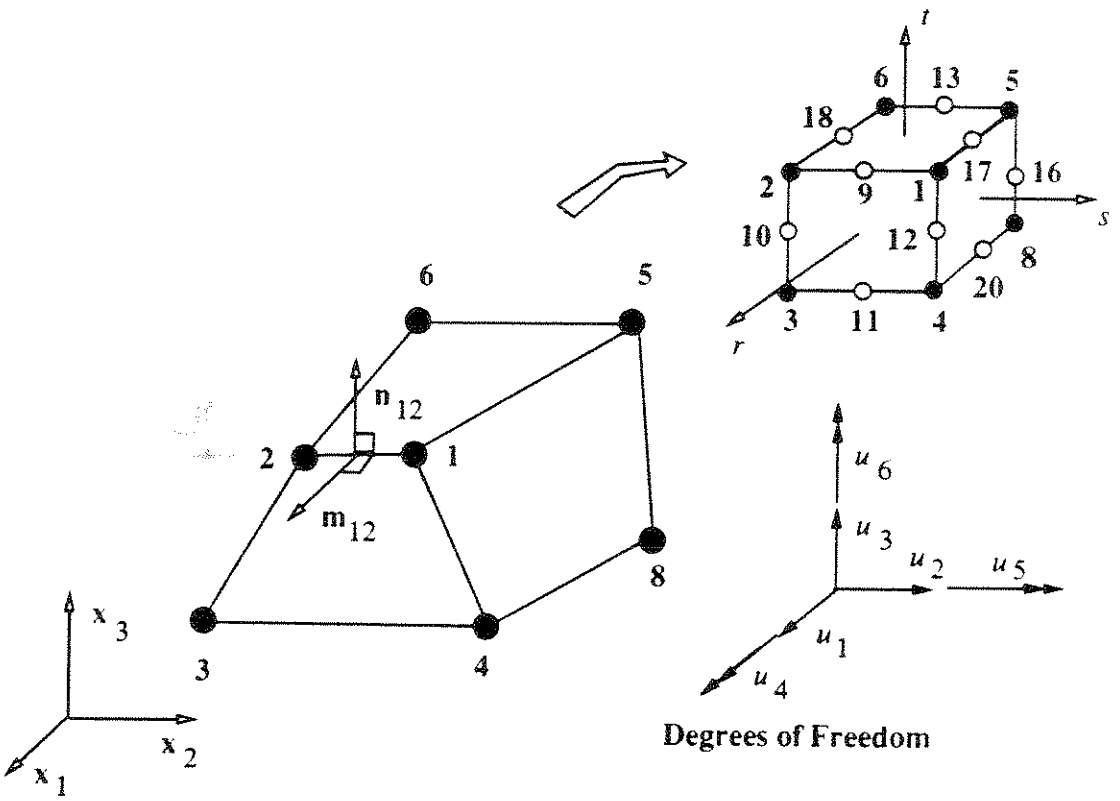

Figure 1.- Solid Element with Rotational Degrees of Freedom

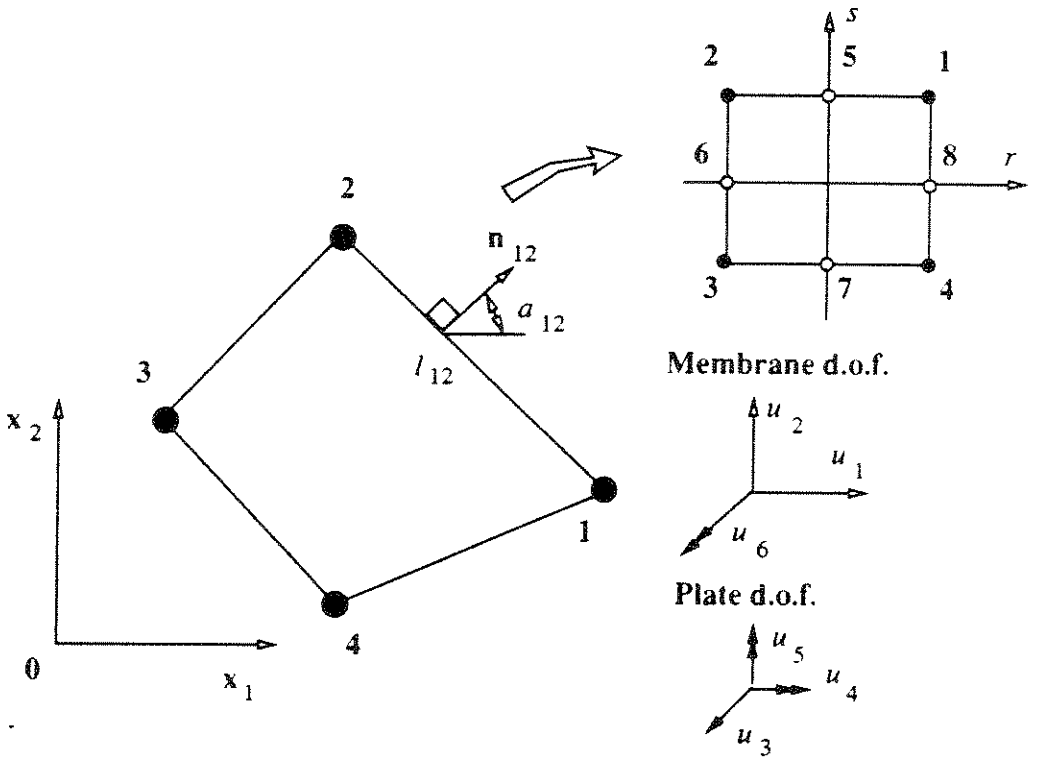

Figure 2. - Thick Flat Shell Element with Drilling Degrees of Freedom

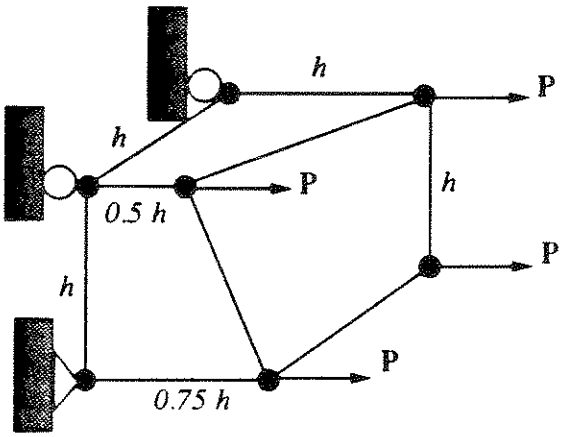

Figure 3. - A Single Element Patch Test for Solid Element

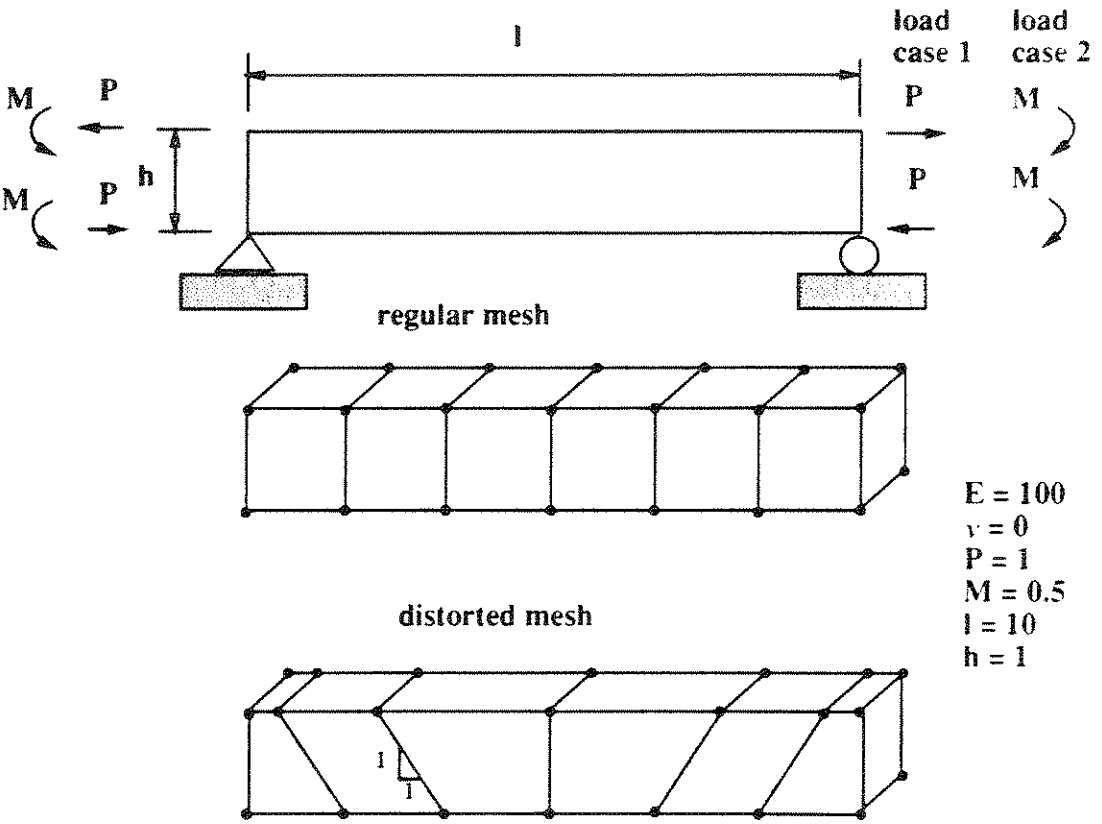

Figure 4. - A Simple Beam

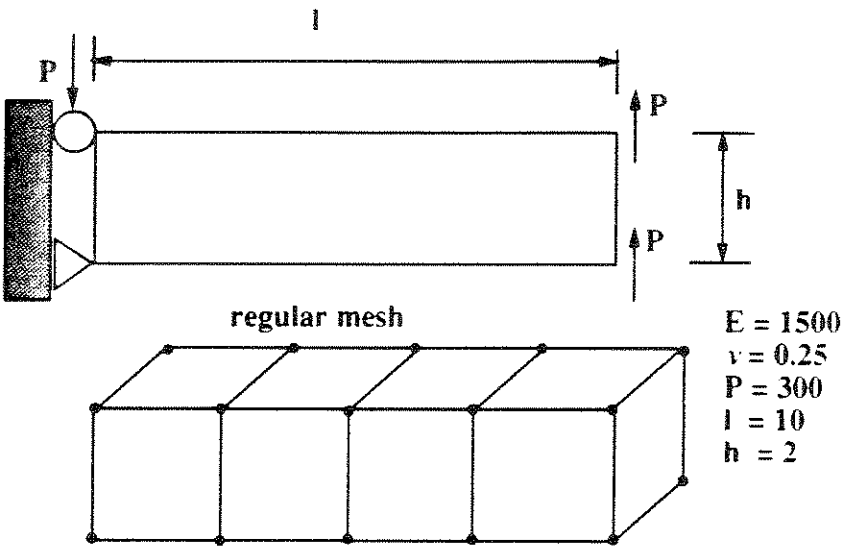

Figure 5. - Short Cantilever Beam

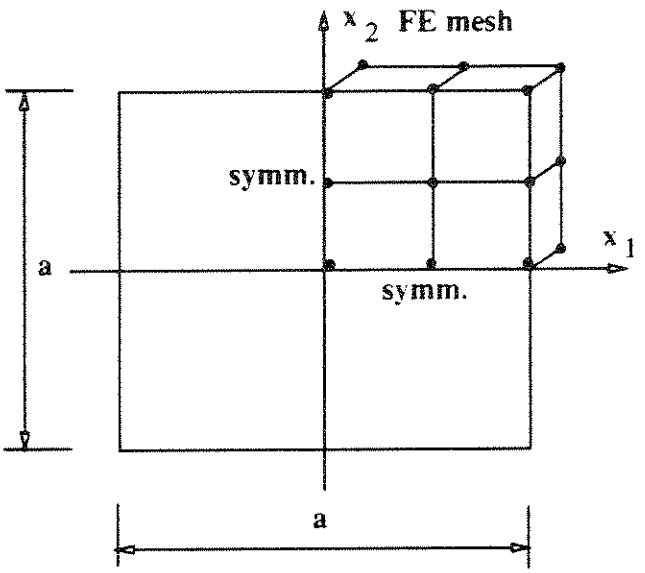

Figure 6. - Simply Supported Square Plate with Uniform Loading

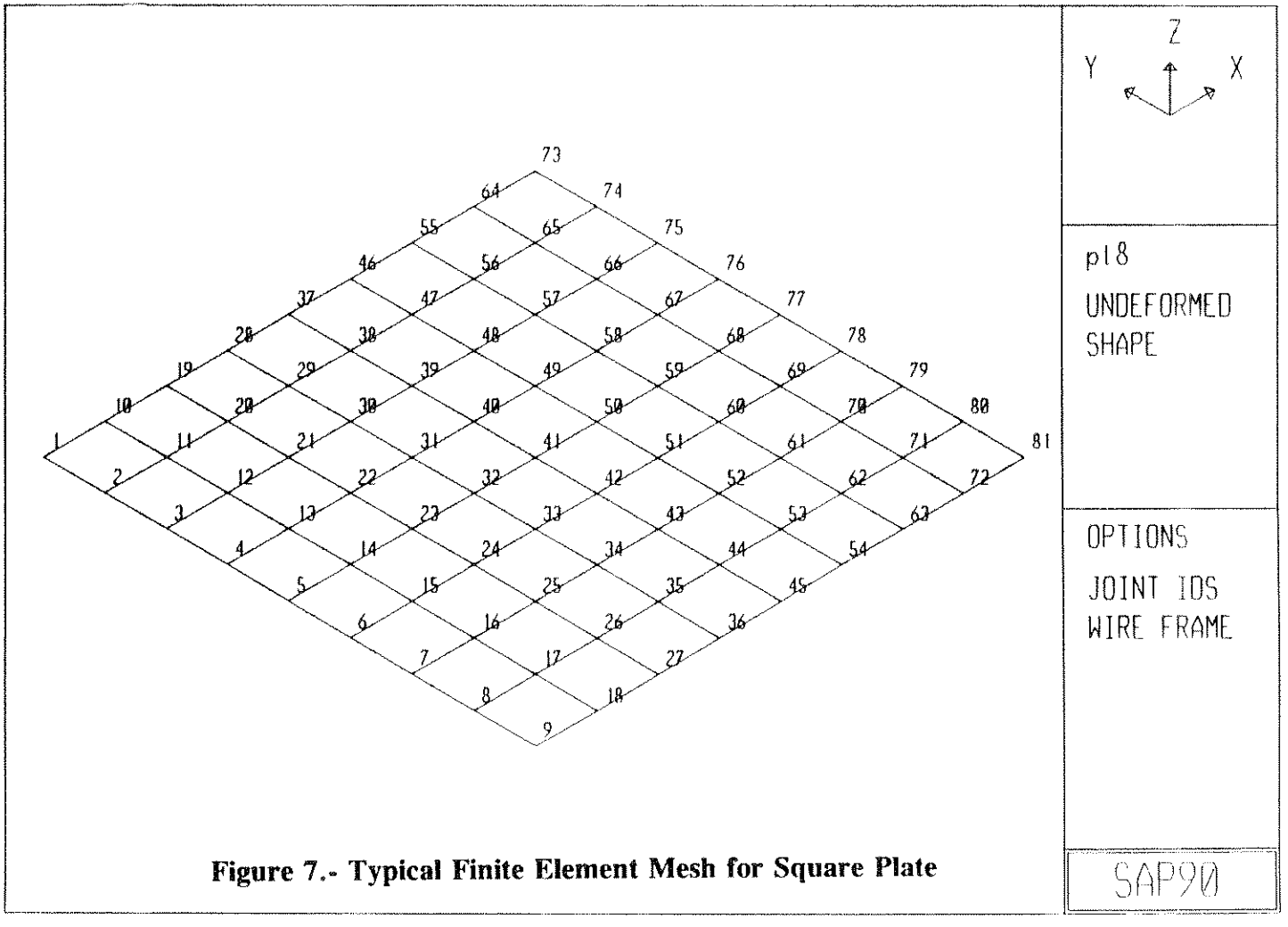

Figure 7.- Typical Finite Element Mesh for Square Plate

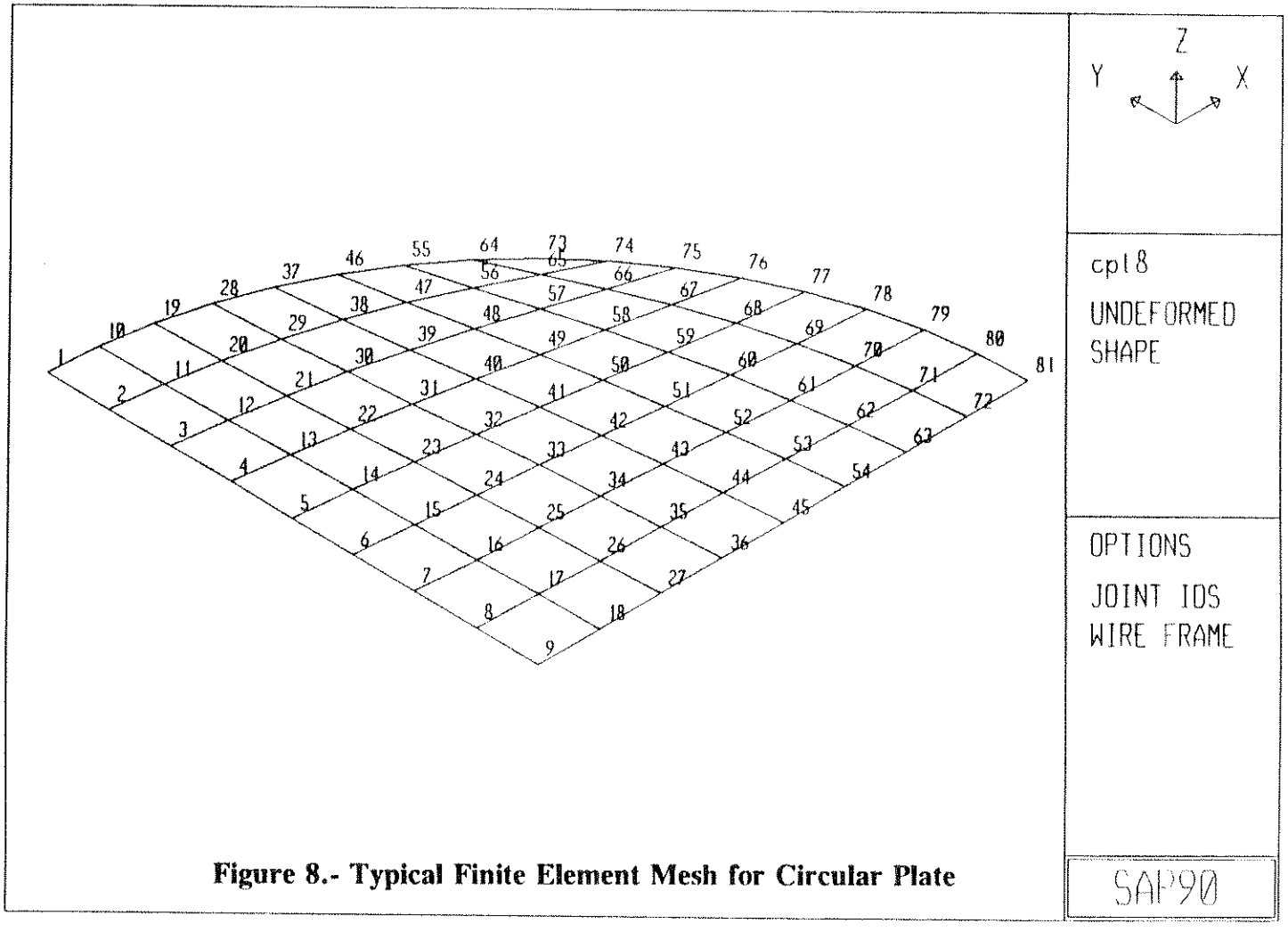

Figure 8.- Typical Finite Element Mesh for Circular Plate

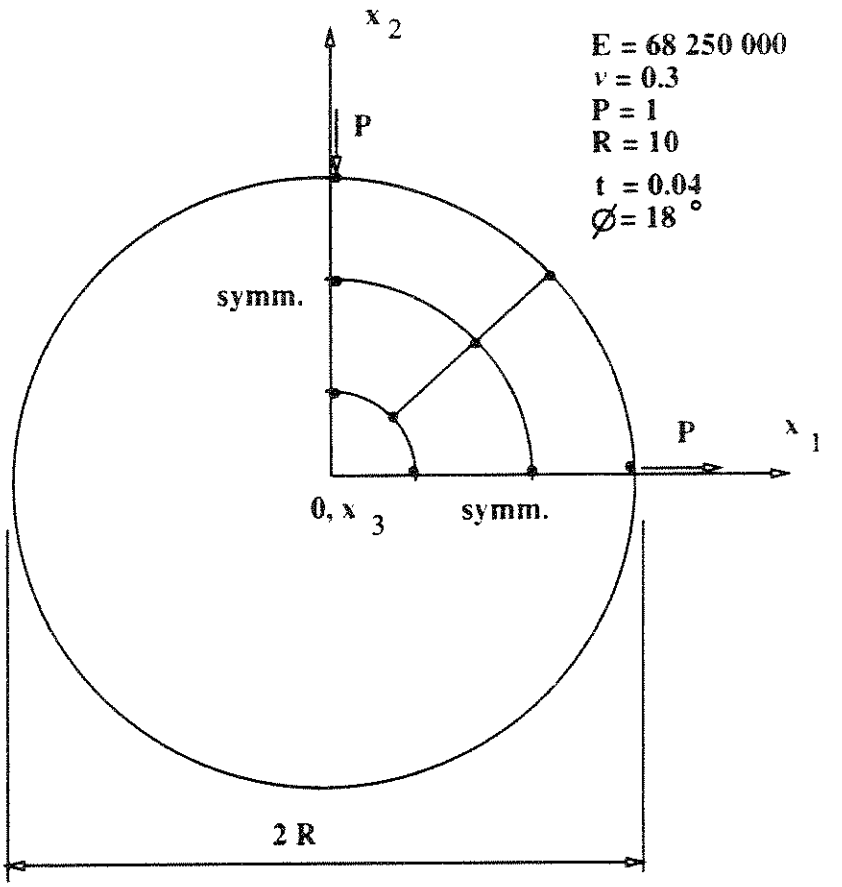

Figure 9. - Pinched Hemisphere with Hole

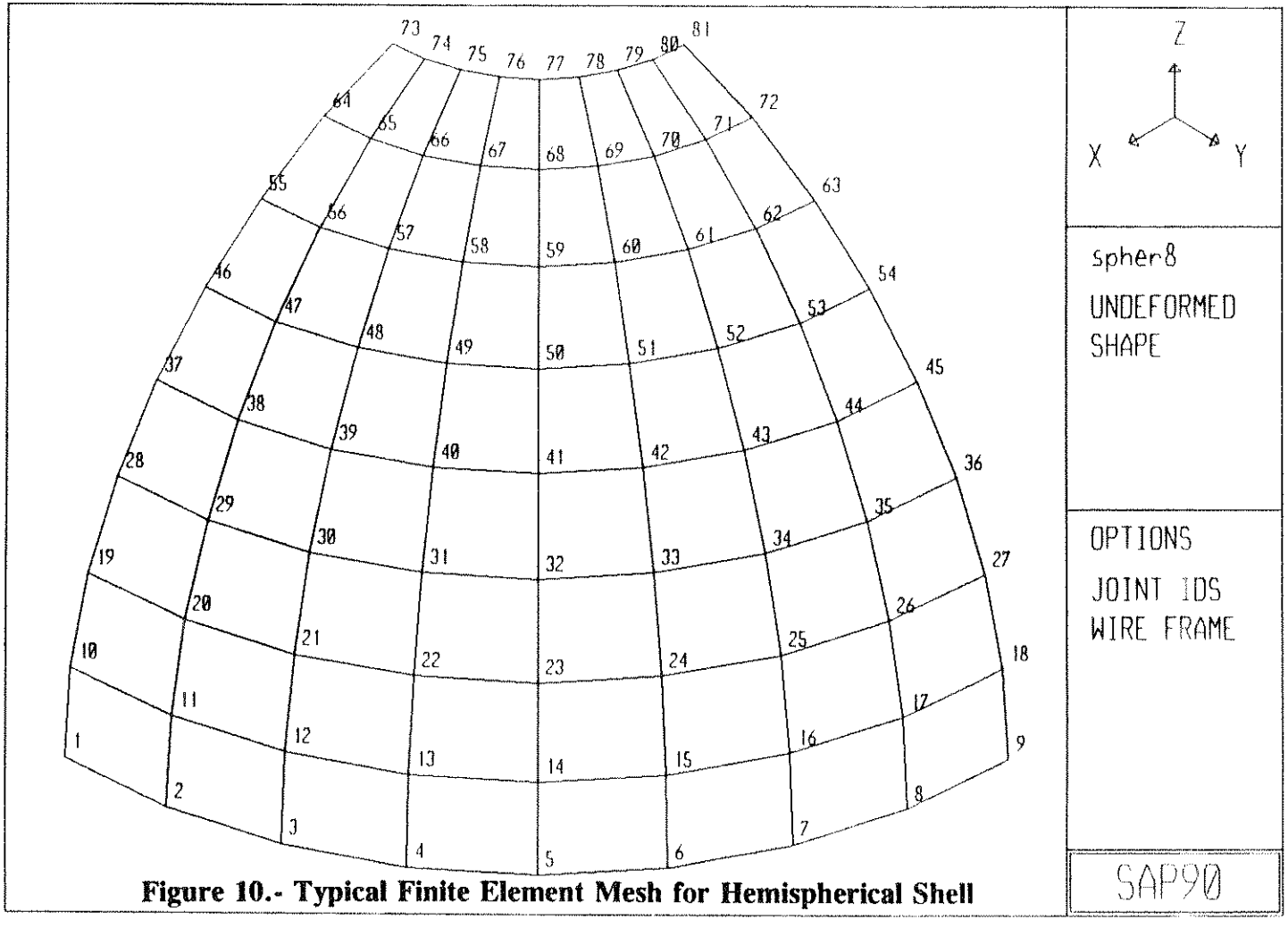

Figure 10.- Typical Finite Element Mesh for Hemispherical Shell